PCCP

Accepted Manuscript

This is an *Accepted Manuscript*, which has been through the Royal Society of Chemistry peer review process and has been accepted for publication.

Accepted Manuscripts are published online shortly after acceptance, before technical editing, formatting and proof reading. Using this free service, authors can make their results available to the community, in citable form, before we publish the edited article. We will replace this *Accepted Manuscript* with the edited and formatted *Advance Article* as soon as it is available.

You can find more information about *Accepted Manuscripts* in the **Information for Authors**.

ROYAL SOCIETY OF CHEMISTRY

www.rsc.org/pccp

Journal Name

ARTICLE

Collecting meaningful early-time kinetic data in homogeneous catalytic water oxidation with a sacrificial oxidant

James W. Vickers,[a] Jordan M. Sumliner,[a] Hongjin Lv,[a] Mike Morris,[b] Yurii V. Geletii,[a*] and Craig L. Hill[a*]

As the field of water oxidation catalysis grows, so does the sophistication of the associated experimental apparatuses. However, problems persist in studying some of the most basic aspects of catalytic water oxidation including acquisition of satisfactory early-reaction-time kinetics and rapid quantification of O_2 concentration. We seek to remedy these problems and through better experimental design, elucidate mechanistic aspects of catalytic water oxidation with theory backed by experimental data. Two new methods for evaluating homogeneous water oxidation catalysts by reaction with a stoichiometric oxidant are presented which eliminate problems of incomplete fast mixing and O_2 measurement response time. These methods generate early-reaction-time kinetics that have previously been unavailable.

Introduction

Experimental design of apparatuses to quantify the performance of water oxidation catalysts (WOC) can be challenging since, the product requiring quantification (O_2) is abundant in air. As a testament to this, apparatuses widely vary between groups in this field, meaning that there is no clear best method, and each laboratory set-up has its limitations which can result in systematic errors. These apparatuses are also limited by what type of information one intends to collect; systems designed to quantify O_2 production do not allow for the monitoring of sacrificial oxidant consumption and vise-versa. By virtue of the experimental design, simultaneous monitoring of O_2 formation and oxidant consumption has not been possible. Most kinetic data for WOC systems are the result of separate experiments and experimental setups. In our early work in this field, we would add the sacrificial oxidant to the WOC solution via cannula transfer, then monitor the O_2 final yield by gas chromatography (GC), whereas sacrificial oxidant consumption kinetics were obtained using a stopped-flow apparatus. Other groups have reported evaluating WOCs by a variety of mixing methods, including injecting solutions into one another by pipette or syringe.[1-14] Heavily linked to the experimental design is the O_2 detection method, which also varies from group to group as each one has inherent strengths and weaknesses. Here we report a new experimental design that takes advantage of detection method strengths while avoiding the weaknesses in the pursuit of a more accurate mechanistic understanding of WOCs.

The reaction mechanism is a working hypothesis to predict a rate law that agrees with experimental results. However, if a mechanism agrees with the experimental results, this does not mean that the mechanism is correct. Different reaction mechanisms can result in the same rate law with respect to one or more of the reactants. With comprehensive kinetic studies, the number of possible mechanisms can be restricted and ideally reduced to just one by. Complicating the process, the concentrations of reagents are not measured directly in most cases, therefore a correct interpretation of raw kinetic data becomes imperative. We further our new experimental design by describing and discussing the interpretation of kinetic data for the reaction of catalytic water oxidation by the stoichiometric oxidant, $[Ru(bpy)_3]^{3+}$ (henceforth Ru^{3+}). These reactions are rather fast at neutral pH values (typical time scales are seconds) and the determination of both O_2 evolution and Ru^{3+} consumption for the same reaction at the same time is reported. The ability to follow both reactant and product (O_2) with time on short timescales is unprecedented. Additional problems with quantification of Ru^{3+} concentration by UV-vis spectrophotometry are addressed including precipitate of Ru^{n+} salts of the WOC.

Experimental

Materials and Methods.

Synthesis. $[Ru(bpy)_3]Cl_2$, sodium persulfate, $Co(NO_3)_2 \cdot 6H_2O$, and all other reagents were obtained from commercial sources. $[Ru(bpy)_3]Cl_2$ was recrystallized prior to use. $[Ru(bpy)_3](ClO_4)_3$, $Na_{10}[Co_4(H_2O)_2(PW_9O_{34})_2]$ (**Co₄POM**),[13] and $Rb_8K_2[(Ru_4O_4(OH)_2(H_2O)_4)(\gamma\text{-}SiW_{10}O_{36})_2]$ (**Ru₄POM**)[11] were prepared as previously described.

Instruments. Water oxidation with $[Ru(bpy)_3]^{3+}$ was performed using a Hi-Tech KinetAsyst Stopped Flow SF-

61SX2 instrument equipped with a diode array detector operating in wavelength range 400-700 nm. In a typical experiment one of the syringes was filled with a $Ru(bpy)_3^{3+}$ solution, and the other with a buffered solution of WOC. The consumption of $Ru(bpy)_3^{3+}$ was followed by a decrease in absorbance at 670 nm ($\varepsilon_{670} = 4.2 \times 10^2$ M^{-1} cm^{-1}) with optical path length $l = 10$ mm. Detailed analysis of kinetic data was performed using both Copasi 4.7 (Build 34).[15]
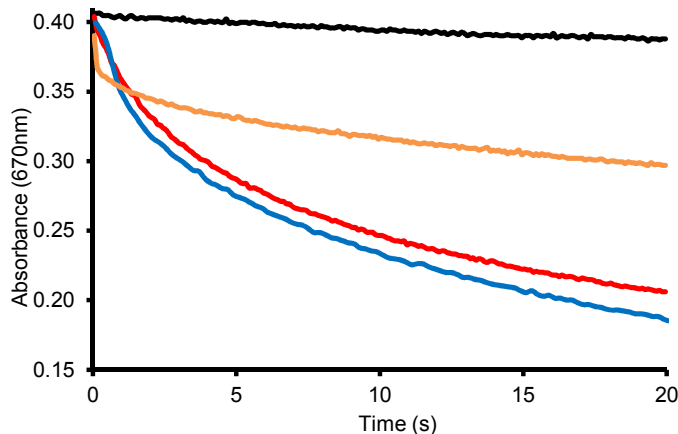

Fig. 1. Kinetic curves of decrease in absorbance at 670 nm obtained by stopped-flow technique. Conditions: 25 ºC, 1.0 mM Ru^{3+}, 40 mM NaP_i, pH = 8.0, no catalyst (black), 3 µM **Ru₄POM** (orange), 3 µM **Co₄POM** (red) and 5 µM $Co(NO_3)_2$ (blue).

Fast Mixing System. Quantification of O_2 was performed using A Hi-Tech Scientific SF-61SX2 mixing apparatus. Stock solutions at twice the desired final concentrations were deareated with Ar in round bottom flasks before being injected into the mixer with 1010 TLL Gastight Hamilton syringes. One of the feeding syringes was filled with a $Ru(bpy)_3^{3+}$ solution and the other with a freshly prepared solution of WOC in buffer. The mixing apparatus was connected with PEEK tubing to an Ocean Optics FOXY-FLOW-CELL fitted with an oxygen probe. All joints were sealed with Teflon tape and DAP BLUESTIK adhesive putty. Oxygen measurements were made using an Ocean Optics Neofox Phase Measurement System with a FOXY-R probe and FOXY-AF-MG coating. The probe was calibrated using a two point curve (0 and 20.9%). Repeated shots were performed until the oxygen reading was constant for three shots. The mixer is then purged with deaerated water before the procedure is repeated at least twice more.

Flow System. The flow system is pictured in Scheme 1. Separate solutions of $[Ru(bpy)_3]^{3+}$ in dilute HCl and WOC in buffer were deaerated with Ar in 50 mL vials which feed directly into separate 5 mL syringe pumps. The syringe pumps were controlled with FIA Labs software allowing for movement of the valve and adjusting flow speed. At the beginning of a run, the solutions were drawn into the syringes and simultaneously pumped into a Y-joint where they are quickly mixed. A similar fast mixing procedure has been reported.[16] The mixed solution then flowed through a length of PEEK tubing, which is proportional to the reaction time. The reacted solution then flowed through a Z-cell with 1 cm path-length and optical glass windows. Fiber optics were attached to the cell and run to an Ocean Optics UV-vis 2000+ and a LS-1 tungsten lamp respectively. The solution then passed through a short length of tubing to a T-cell with a FOXY-R oxygen sensing probe and finally

to waste. All joints were sealed with Teflon tape and DAP BLUESTIK adhesive putty.

Results and discussion

First, we discuss the importance of fast mixing stock solutions for a reliable determination of O_2 yield for the processes with a reaction time shorter than 1-3 s. Second, we describe a continuous flow technique to follow the kinetics of O_2 formation for fast water oxidation reactions. Under minimally optimized conditions we achieved a resolution shorter than 2 s. Lastly, we discuss typical problems in interpretation of raw kinetic data.

Fast mixing of solutions

Catalytic WOC reactions can be quite fast, especially at basic pH values. For example, when Ru^{3+} is the stoichiometric oxidant, consumption of $Ru^{3+} > 20\%$ is achieved in less than 2 s when **Co₄POM** is used under conditions in Figure 1. Therefore, fast and thorough mixing of stock solutions is required to achieve a homogeneous solution on a timescale short enough to allow for accurate kinetic measurements. Commonly, one solution is simply injected into another without special care for fast or uniform mixing.[1-14] In these cases high local concentrations of reagents cannot be avoided due to inadequate mixing. Under our previous stoichiometric oxidant mixing procedure, the injection lasted at least 0.5 s preventing kinetic measurement and facilitating determination of only final O_2 yields. After injection, an uneven distribution of color was clearly visible for a short time (the mixing time is estimated to be about 1 s). This is a problem that has plagued the water oxidation literature.
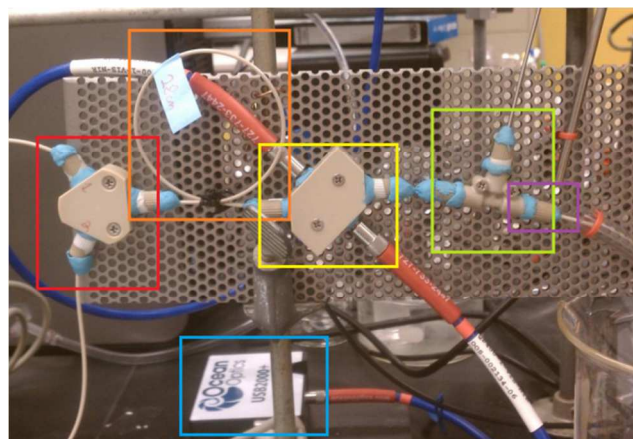
Scheme 1. Continuous flow system comprising (from left to right) two syringe pumps with variable pump volume (out of picture), a Y-mixing joint (red), variable loop of PEEK tubing (orange), a Z-cell with optical glass windows connected to fiber optics (yellow) connected to a tungsten lamp and Ocean Optics UV-vis (blue), and Ocean Optics FOXY optical oxygen probe in a T-cell (green). Teflon tape and DAP Blue Stik adhesive putty used to seal joints (violet).

In our recent work at elevated pH, we use a fast mixing unit from a stopped flow instrument with a mixing time of about 1 ms to ensure fast and consistent mixing.[17] The feeding syringes are filled with deaerated stock solutions, and are pumped through a stopped-flow mixer to a holding chamber where they are stored until the reaction is complete. The mixed solution then flows through a T-joint with O_2 sensor (the same as that used in the continuous flow set up

below). This requires approximately 10-15 shots to obtain a stable reading.

Measurements of O_2 concentration

Measurements of O_2 formation in the present study were obtained with a luminescent oxygen sensor. Optical oxygen sensors do not consume oxygen, do not require frequent calibration and are convenient to use. Due to the presence of Ru^{2+} in solutions which gives a false positive, the probe is coated to prevent light leaking which increases the response time to about 30 seconds. Since no head space is present in the setups described here, we did not need to consider the mole fraction of O_2 in the gas phase. The calibrations of the optical probes are stable regardless of media, stirring speed and other variable experimental conditions.[18-20] Clark style electrodes have known disadvantages[4, 8, 18, 20, 21] despite their wide usage in the literature.[3, 4, 8, 18] They consume oxygen, and therefore their signal is proportional to the rate of O_2 diffusion past the oxygen permeable membrane, through the electrolyte solution and to the electrodes where O_2 is reduced to OH^-. As a result, the signal depends on multiple factors including the stirring speed, hydrodynamics of the sensor geometry, and is prone to drift from surface contamination and change in the alkalinity of the electrolyte over time. Thus, the calibration should be done under exactly the same conditions in the narrow range of O_2 concentrations. Micro electrodes can be used to obtain faster response time, at the expense of lower measured currents, and still have a response time of 2-3 seconds. One shared disadvantage of both approaches is that they are temperature dependent, and when only small amounts of O_2 are produced, control of the temperature is critical. Gas chromatographic analysis of the reactor head space remains the ultimate technique to confirm the presence of O_2 and to quantify the amount of oxygen leaked from air into the reactor, but again, the response time of this technique is too slow for monitoring kinetics. Finally worth mention here are manometric measurements of O_2 formation seem to be close to ideal, but in most cases the overall yield of O_2 is too small to detect the change in gas pressure.

Continuous flow technique

Monitoring the fast kinetics of both O_2 yield and consumption of oxidant remains an experimental challenge. For the continuous flow system described in this work, the reaction time is the ratio of the loop volume (orange square in Scheme 1) and the flow rate, eq 1.

$$\text{Reaction Time (s)} = \frac{\text{Volume } (\mu L)}{\text{Flow Rate } (\frac{\mu L}{s})} \qquad (1)$$

The desired reaction time can be achieved by varying the flow rate and the loop volume. At current configuration the shortest reaction time achievable is 0.75 s and the variable flow rate of the pumps allows for two orders of magnitude change in reaction time. Because the two pumps contain a total of 10 mL of solution, the O_2 probe and UV-vis are able to continuously observe the reaction time of 0.75 s for 10 s. While this is still slightly faster than the response time of the coated optical probe, experiments can be run in immediate succession, thus eliminating any concerns regarding the response time of the probe.

Furthermore, the continuous flow system presented here is able to collect both O_2 kinetic data, and Ru^{3+} consumption kinetics for the same reaction at the same time. Previous studies were limited to examining the reactions at similar conditions but variation in mixing time and method persisted, limiting quantitative comparison. All experimental details of the two methods of measurement in the continuous flow system are identical. However, there exists a slight delay that makes the reaction time observed by the FOXY probe slightly longer than the UV-vis. The length of tubing connecting these two sensors is short (Scheme 1), but does produce a modest delay of at most approximately 1.8 s for the slowest flow rates which, in this case, is about 2% of the total reaction time. An example of data collected in the flow setup is given in Figure 2.

Measurements of $[Ru(bpy)_3]^{3+}$ concentration

While it does have limitations, Ru^{3+} is a common primary oxidant for WOC studies, the most common primary oxidant when the WOC is a POM, and even more so if Ru^{2+} in a light driven system is included. Our recent work contains a table with the conditions of POM WOC studies to date[22] and a recent review examines common primary oxidants in WOC studies in general.[23]

The spectrum of Ru^{3+} has a broad maximum at $\lambda = 670$ nm with $\varepsilon = 420$ $M^{-1}cm^{-1}$, which makes UV-vis spectroscopy an ideal technique to study the kinetics of its consumption. It is often assumed that the concentration of Ru^{3+} is directly proportional to the absorbance based on Beer's law. However, Ru^{2+} has a small absorbance at 670 nm which can become substantial in high concentrations. Decomposition products of Ru^{3+} often absorb near 670 nm as well which can be higher than that of Ru^{2+}.[24] Even the WOC itself can also absorb light at this wavelength which is obvious when **Ru_4POM** is used, and while **Co_4POM** has a very low molar absorptivity, little is known about the spectra of its higher oxidation states during turnover. Without consideration of these overlapping components, this could affect the relationship between Ru^{3+} and the absorbance, especially at high conversion. The initial rates determined as $d[Ru^{3+}]/dt = d(A_{670}/\varepsilon l)/dt$ are less sensitive to the absorbance of reaction products. Therefore, one could expect the reaction rate law can be determined from a dependence of initial rates on catalyst and Ru^{3+} concentrations. However, in numerous cases the initial rate cannot be determined due to unique kinetic features of a given WOC, as evident from the data in Figure 1. The initial rates for the reaction catalyzed by **Ru_4POM** are very high and strongly depend on traces amounts of Ru^{2+} present in solution as has been previously elaborated.[25] A similar scenario is operable when Co^{2+} (aq) is employed as the catalyst: there is an induction period which has been addressed in several recent publications.[26, 27] No special features are seen for the system with **Co_4POM** in Figure 1 (red curve, the conditions are the same as in recently published paper).[10] Thus, at short time scales it is quite clear that the kinetic curve cannot be approximated by a straight line. Only the fitting of whole kinetic curves "A_{670} vs. time" could provide valuable information on kinetics of Ru^{3+} consumption.
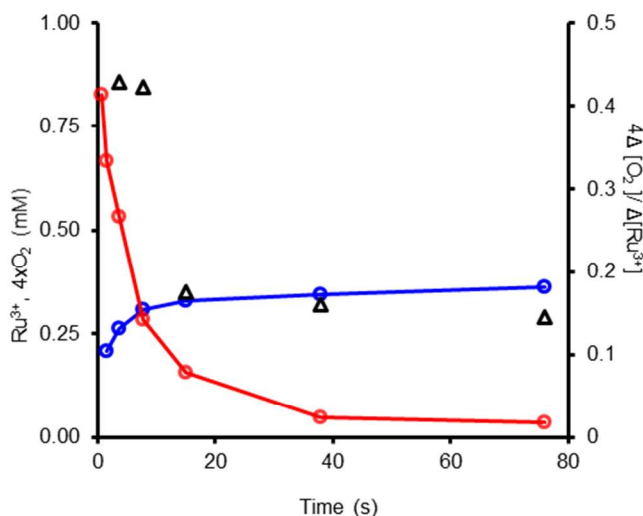
Fig. 2. Kinetics of 1.2 mM Ru^{3+} consumption (red) and $4xO_2$ formation (blue) in 60 mM NaP_i at pH 7.2 in the presence of 8 μM **Ru_4POM** and selectivity $(4x\Delta[O_2]/\Delta[Ru^{3+}]$, black) collected by the continuous flow technique.
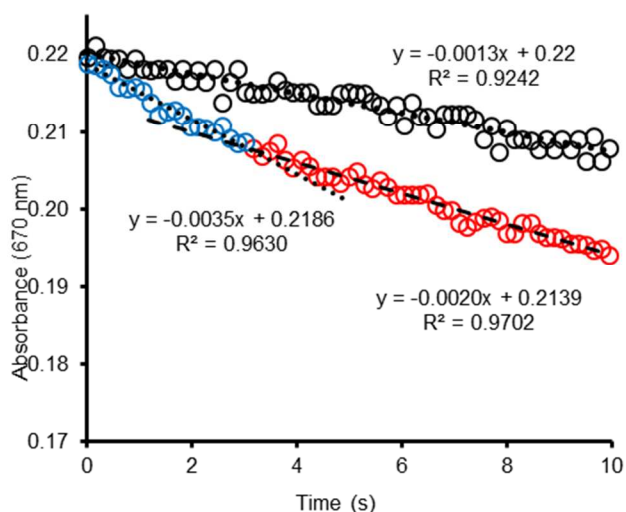

Fig. 3. Kinetic curves of decrease in absorbance at 670 nm obtained by stopped-flow technique. Conditions: 25 ºC, 0.5 mM Ru^{3+}, 0.1 mM Ru^{2+}, 30 mM NaP_i, pH = 7.2 without catalyst (black) and with 1.0 μM **Co_4POM** 1-3 seconds (blue) 3-10 seconds (red). The solution of Ru^{3+}/Ru^{3+} (pH~3) was mixed with the solution of the catalyst in buffer.

Recently Stracke and Finke collected the kinetics of both Ru^{3+} consumption (absorbance at 675 nm) and O_2 formation (by a custom made Clark microelectrode) for the reaction of water oxidation by Ru^{3+} in 30 mM phosphate buffer (pH 6.5-7.8) catalyzed by **Co_4POM**.[10] The reaction rate law was determined based on measurement of initial reaction rates. The stock solutions were mixed by pipette injection, and the absorbance was measured each second using a diode-array UV-vis spectrophotometer. The initial rate was measured at ~10% conversion typically within the first 10 s. Our measurements under the same standard experimental conditions but using a stopped flow technique revealed that the initial part of the kinetic curves cannot be approximated by a straight line, Figure

3. The reaction within the initial 3 s is almost twice as fast as the rate determined in the time range 3-10 s. This seems to also be true under other experimental conditions. In the procedure described by Stracke and Finke the kinetic measurements most likely start 2-3 seconds after the beginning of the reaction. Consequently, instrumental limitations only permitted measurements after this amount of time. The beginning of the kinetic curve might be due to an establishment of steady state conditions.
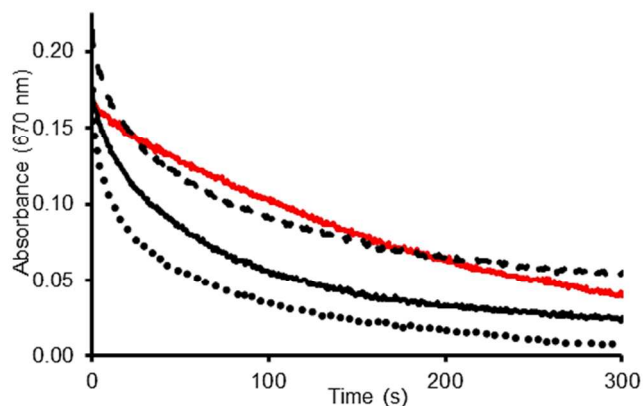

Fig. 4. Kinetic curves of decrease in absorbance at 670 nm obtained by stopped-flow technique. Conditions: 25 ºC, 0.4 mM Ru^{3+}, 0.1 mM Ru^{2+}, 30 mM NaP_i, pH = 7.2 without catalyst (red) and with 3.0 μM **Co_4POM** (black lines). The solution of Ru^{3+} (pH~3) was mixed with the solution of **Co_4POM** and Ru^{2+} in buffer aged 4 hours (dashed black). The solution of Ru^{3+} and Ru^{2+} (pH~3) was mixed with the solution of **Co_4POM** in buffer aged 5-15 min (solid black line). **Co_4POM** added to Ru^{3+} with no initial Ru^{2+} (dotted black).

The effect of precipitation on the reaction kinetics.

Previously, we reported that an initially homogeneous mixture of Ru^{3+} with **Co_4POM** became cloudy before reaction completion.[13] Such behavior indicates that the solubility of the POM complex with Ru^{2+} is lower than that with Ru^{3+}. This property has been used to precipitate POM complexes from solution by adding more Ru^{2+}.[13] Recently, the solubility constant of $(Co_4POM)_2(Ru^{2+})_3$ has been determined in 30 mM sodium phosphate (NaP_i) buffer: $K_{sp} = (8 \pm 7) \times 10^{-25}$ (M^5).[10] In the presence of 0.5-1.0 mM Ru^{2+} the concentration of **Co_4POM** was estimated to be very low, ~ 10^{-7} M. Based on this value, kinetics data were analyzed assuming that **Co_4POM** in solution is in equilibrium with the insoluble complex.[10] However, the process of precipitation is often kinetically controlled and strongly dependent on ionic strength. For a relatively fast reaction, the post-reaction solution could be homogeneous but supersaturated. Under such conditions, the low solubility of the reaction products might not affect the reaction kinetics. Experimentally, precipitation is visible as an increase of background absorbance in UV-vis spectra due to light scattering. Here, we confirm that the reaction kinetics followed by absorbance at 670 nm strongly depend on the sequence of reagent mixing. This effect is best seen at higher catalyst concentration and is shown in Figure 4. In this experiment, one feeding syringe was filled with fresh Ru^{3+} solution and the second one with **Co_4POM** premixed with Ru^{2+} in phosphate buffer. The second solution was aged about 4 hours before reaction. Both the initial and final absorbencies are significantly higher when catalyst was used (black dashed line) than in the uncatalyzed reaction (red line). When both Ru^{3+} and Ru^{2+} were in the first feeding syringe, and **Co_4POM** was not premixed with Ru^{2+}, the rate of precipitation was slower than the reaction, and no significant increase in background absorbance was detected (solid black line). Thus, a correct design of

the experiment minimizes the effect of low product solubility. In some systems catalyst decomposition may result in formation of catalytically active nanoparticles which may visually appear homogeneous. Developing methods for differentiation between homogeneous and heterogeneous catalysts formed during reaction is an ongoing concern of all homogeneous catalysts,[28-30] and was recently described for this specific system.[10, 27, 31, 32]
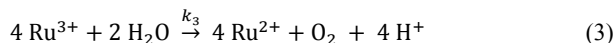
Simplified reaction mechanism.

In order to precisely describe the experimental kinetics data, a reaction mechanism may include numerous steps. Some of them are kinetically insignificant but required to maintain a reaction stoichiometry, charge balance, etc. As a general rule the number of steps in a mechanism should be minimal. Some reactions in a mechanism are not necessarily elementary and may proceed in several simpler steps, however, these are very fast and are described by apparent reaction rate constants.
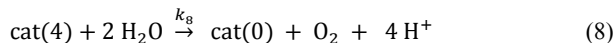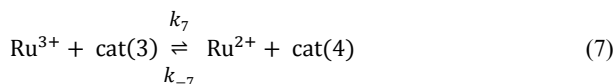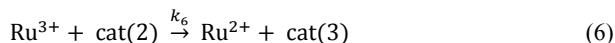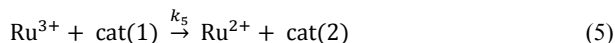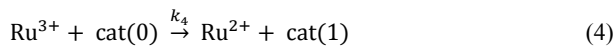
In stoichiometric water oxidation, Ru^{3+} is a commonly used oxidant and has a standard oxidation potential 1.21 V (NHE).[23, 33] It is rather stable under acidic conditions, but in neutral and basic conditions Ru^{3+} undergoes self-decomposition in "eq 2" with the rate dependent on pH and the nature and concentration of buffer. The decay kinetics are first order and the rate constant k_2 is 0.0014 s^{-1} in Na_2SiF_6-$Na_2B_4O_7$ at pH ca 5.5,[34] 0.02 and 0.05 s^{-1} in borate buffer at pH 8 and 9, respectively.[35, 36] This is for a generic reaction (eq. 2) where one or more of the bpy ligands are oxidized one or more times; some of the bpy ligand is fully oxidized to CO_2, however, the products are largely $[Ru(bpy)_3]^{2+}$ with the yield up to 98% based on initial Ru^{3+}. Sutin *et al.* have identified at least eight separate products in previous work.[24] Despite this previous work, little is known about the importance of these reactions and the rates relative to water oxidation.

$$Ru^{3+} \xrightarrow{k_2} products \quad (2)$$

In the presence of WOC four oxidative equivalents of Ru^{3+} are used to oxidize water in eq 3.

$$4\,Ru^{3+} + 2\,H_2O \xrightarrow{k_3} 4\,Ru^{2+} + O_2 + 4\,H^+ \quad (3)$$

The simplified mechanism of catalytic water oxidation is given in eqs 4-8:

$$Ru^{3+} + cat(0) \xrightarrow{k_4} Ru^{2+} + cat(1) \quad (4)$$

$$Ru^{3+} + cat(1) \xrightarrow{k_5} Ru^{2+} + cat(2) \quad (5)$$

$$Ru^{3+} + cat(2) \xrightarrow{k_6} Ru^{2+} + cat(3) \quad (6)$$

$$Ru^{3+} + cat(3) \underset{k_{-7}}{\overset{k_7}{\rightleftharpoons}} Ru^{2+} + cat(4) \quad (7)$$

$$cat(4) + 2\,H_2O \xrightarrow{k_8} cat(0) + O_2 + 4\,H^+ \quad (8)$$

where "i" in cat(i) is the number of electrons removed from the resting oxidation state of a catalyst. The first three reactions are assumed to be fast and the [cat(0)], [cat(1)], [cat(2)], [cat(3)], [cat(4)] to be steady state. Under these assumptions, and taking into account the mass balance for total catalyst concentration [cat], the rate law of Ru^{3+} consumption is in eq 9, for which a detailed derivation is provided (see ESI):

$$\frac{-d[Ru^{3+}]}{dt} = k_2[Ru^{3+}] + \frac{4k_8k_7[Ru^{3+}][cat]}{(k_7[Ru^{3+}] + k_{-7}[Ru^{2+}] + k_8)} \quad (9)$$

For illustration purposes we simplify eq 9.

If $k_7[Ru^{3+}] + k_{-7}[Ru^{2+}] \ll k_8$ then the reaction in eq 7 is the rate limiting step and the reaction rate laws are eq 10a-10b:

$$\frac{-d[Ru^{3+}]}{dt} = k_2[Ru^{3+}] + 4k_7[Ru^{3+}][cat] \quad (10a)$$

$$\frac{d[O_2]}{dt} = k_7[Ru^{3+}][cat] \quad (10b)$$

In this case the O_2 yield per consumed Ru^{3+} is eq 11:

$$\frac{-d[O_2]}{d[Ru^{3+}]} = \frac{k_7[cat]}{(k_2 + 4k_7[cat])} \quad (11)$$

At high concentration of the catalyst the contribution of the reaction in eq 2 is negligible and O_2 yield should be equal to $(1/4)[Ru^{3+}]_o$. However, this scenario is not consistent with experimental data (see below). If $(k_{-7}[Ru^{2+}] + k_7[Ru^{3+}]) \gg k_8$, the reaction in eq 7 is equilibrated, $K_7 = k_7/k_{-7}$, and rate laws are eqs 12a-12b:

$$\frac{-d[Ru^{3+}]}{dt} = k_2[Ru^{3+}] + \frac{4k_8K_7[Ru^{3+}][cat]}{([Ru^{2+}] + K_7[Ru^{3+}])} \quad (12a)$$

$$\frac{d[O_2]}{dt} = \frac{k_8K_7[Ru^{3+}][cat]}{([Ru^{3+}] + K_7[Ru^{3+}])} \quad (12b)$$

$$\frac{-d[O_2]}{d[Ru^{3+}]} = \frac{k_8K_7[cat]}{(k_2([Ru^{2+}] + K_7[Ru^{3+}]) + 4k_8K_7[cat])} \quad (13)$$

Taking into account that $[Ru^{2+}] \approx ([Ru^{3+}]_o - [Ru^{3+}])$, eq 13 can be simplified to eq 14, which after integration gives eq 15:

$$\frac{-d[O_2]}{d[Ru^{3+}]} = \frac{k_8K_7[cat]}{(k_2[Ru^{3+}]_o + k_2(K_7-1)[Ru^{3+}] + 4k_8K_7[cat])} \quad (14)$$

$$\frac{[O_2]}{[Ru^{3+}]_o} = \left\{ \frac{\left(\frac{0.25\,k_8K_7[cat]}{k_2}\right)}{(K_7-1)} \right\} \ln\left\{ 1 + \left(\frac{K_7-1}{[Ru^{3+}]_o + 4k_8K_7\frac{[cat]}{k_2}} \right) \right\} \quad (15)$$

The analysis of eq 15 reveals that O_2 yield per $[Ru^{3+}]_o$ quickly reaches 100% with increase of [cat] and weakly dependent on $[Ru^{3+}]_o$, which is again not consistent with experimental data. This inconsistency between the simple kinetic model and experimental results indicate that there exists a catalytic pathway of Ru^{3+} decomposition, thus the model must be expanded to incorporate additional Ru^{3+} decomposition steps.† Recently the same conclusion has been made by Finke.[10]

Selectivity of the catalyst.

At high catalyst concentration the O_2 yield based on $[Ru^{3+}]_o$ concentration, $4x[O_2]/[Ru^{3+}]_o$ should be 100%, but experimentally determined yields are lower (Figure 5), ca 65% for **Ru_4POM**.[11,23] A similar phenomenon was observed for the IrO_2 catalyst.[34] The lower than expected O_2 yield can be explained by a catalytic oxidation of bpy ligand in the $Ru^{3+/2+}$ complexes, which is explored in-depth by Sutin.*et al.*[24] For the purpose of illustration and simplicity we assume that the bpy ligand is oxidized by cat(4) in eq 16 as it is the strongest oxidant in the system. We also considered the scenario where bpy is oxidized in Ru^{3+} species, but this appeared to be inconsistent with experimental data.
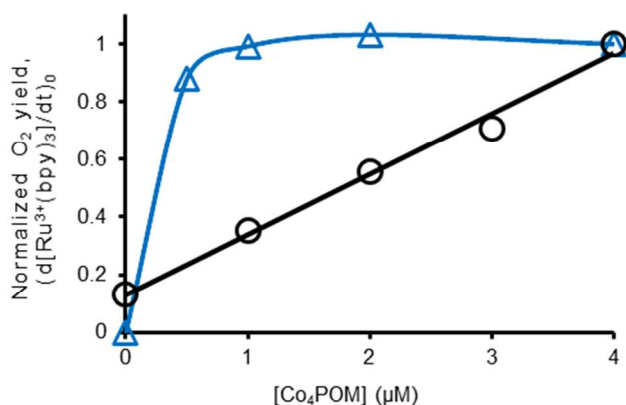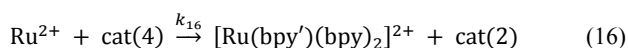
Fig. 5. Normalized O_2 yield (blue triangles) and initial rates of $[Ru^{3+}]$ consumption (black circles) in the reaction of water oxidation by 1.0 mM $[Ru^{3+}]$ in 80 mM sodium borate buffer at pH 8.0. $4 \times [O_2]/[Ru^{3+}]_o = 0.48 \pm 0.05$ at 4 μM **Co₄POM**

$$Ru^{2+} + cat(4) \overset{k_{16}}{\rightarrow} [Ru(bpy')(bpy)_2]^{2+} + cat(2) \qquad (16)$$

where bpy' is a product of bpy oxidation. Such a product is more oxidizable than the initial bpy and therefore triggers a sequence of oxidation reactions up to CO_2 formation as has been quantified previously.[27] For simplicity, these reactions can be written as eq 17, the identity of the products is largely unimportant here.

$$n\, Ru^{3+} + [Ru(bpy')(bpy)_2]^{2+} \overset{k_{17}}{\rightarrow} n\, Ru^{2+} + products \quad (17)$$
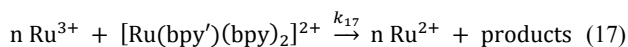
After taking into account the reactions in eqs 16-17 and assuming fast equilibration in eq 6, the rate laws are in eqs 18a-b, and O_2 yield in eq 19:

$$\frac{-[Ru^{3+}]}{dt} = \frac{K_7[Ru^{3+}][cat]\,(4k_8 + nk_{16}[Ru^{2+}])}{([Ru^{2+}] + K_7[Ru^{3+}])} \qquad (18a)$$

$$\frac{d[O_2]}{dt} = \frac{k_8 K_7[Ru^{3+}][cat]}{([Ru^{2+}] + K_7[Ru^{3+}])} \qquad (18b)$$

$$\frac{-d[O_2]}{d[Ru^{3+}]} = \frac{1}{\left(4 + \frac{nk_{16}[Ru^{2+}]}{k_8}\right)} \qquad (19)$$

The validity of eq 19 has been qualitatively confirmed by the data obtained using the continuous flow technique, Figure 2. Indeed, with accumulation of Ru^{2+}, the ratio $\Delta[O_2]/\Delta[Ru^{3+}]$ quickly decreases with time. This is consistent with two competitive reactions involving cat(4); the desired water oxidation in eq 8, and destructive Ru^{2+} ligand oxidation in eq 16. The catalytic oxidation of bpy ligand is also observed in the reaction catalyzed by **Co₄POM**: the final O_2 is twice lower than theoretical and is independent of catalyst concentration (Figure 5). However, the kinetic data do indicate that the same reactive intermediate is involved in both the water and ligand-oxidation reactions. This, in turn, means that the selectivity of the catalyst is controlled primarily by the relative reactivity of this intermediate in eq 8 and eq 16 where the selectivity is a function of $[Ru^{2+}]$, k_{16}, and k_8 as indicated by eq 19. The initial rates of Ru^{3+} consumption are reproducible and do not strongly depend on traces of Ru^{2+} (Figure 1), in contrast to **Ru₄POM**. This would be consistent

with eq 7 being the rate-limiting step. In this case the rate law should be eq 20:

$$\frac{-d[Ru]^{3+}}{dt} = 4k_7[Ru^{3+}][cat] \qquad (20)$$

Indeed, the initial rates are linearly proportional to [cat] (Figure 5), but the kinetics of Ru^{3+} consumption measured as the decrease of absorbance at 670 nm is not exponential (Figure 6). As discussed above this deviation from exponential decay could arise from increase of absorbance by reaction products. Since the equation describing the dependence of $[Ru^{3+}]$ versus time cannot be derived in this case, we performed a digital simulation using Copasi software[15] and the mechanism in eqs 4-8, and 16. The simulation demonstrated that the absorbance of Ru^{3+}, Ru^{2+}, and $[Ru(bpy')(bpy)_2]^{2+}$ should be taken into account to obtain an agreement with experimental data, as discussed above. The simulation gave $4[O_2]/[Ru^{3+}] = 0.52$, which is an excellent agreement with experimental value 0.48. The parameters for simulation are given in Figure 3. Thus, a thorough analysis of limited amount of kinetic data could provide solid evidence for the reaction mechanism. Note that the above reaction mechanism does not require taking precipitation of the catalyst into account. The inhibition of the reaction by Ru^{2+} is explained by the reversibility of eq 7.
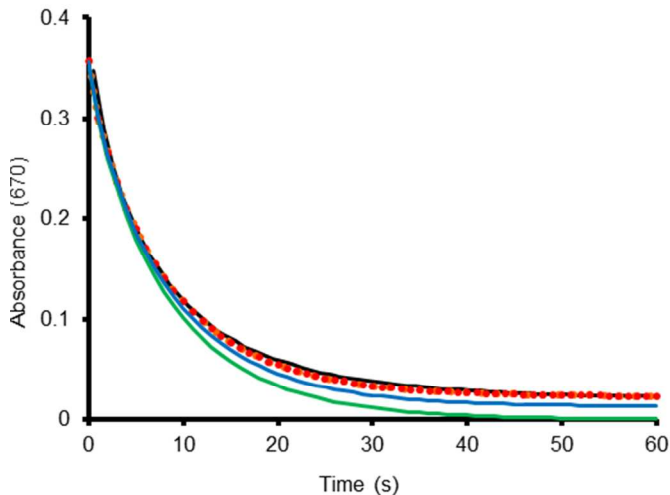

Fig. 6. The experimental (black) and simulated kinetics of decrease of absorbance at 670 nm. Conditions: 0.85 mM Ru^{3+}, 2 μM **Co₄POM**, 80 mM NaB_i buffer at pH 8.0, 25 °C. Parameters used in simulation: $k_4 = k_5 = k_6 = 10^9\ M^{-1}s^{-1}$, $k_7 = 10^5\ M^{-1}s^{-1}$, $k_{-7} = 10^7\ M^{-1}s^{-1}$ $k_8 = 10^5\ s^{-1}$ $k_{16} = 6 \times 10^7\ M^{-1}s^{-1}$, $\varepsilon(Ru^{3+}) = 420\ M^{-1}cm^{-1}$, $\varepsilon(Ru^{2+}) = 20\ M^{-1}cm^{-1}$, $\varepsilon([Ru(bpy')(bpy)_2]^{2+}) = 50\ M^{-1}cm^{-1}$††. Red dotted line: all three extinction coefficients were used. Blue line: $\varepsilon(Ru^{3+})$ and $\varepsilon(Ru^{2+})$ were used. Green line: only $\varepsilon(Ru^{3+})$ was used.

Conclusions

Through our work with WOCs we have come to identify some shortcomings of our own experimental design and those reported in the literature. When O_2 is measured by mixing solutions of $[Ru(bpy)_3]^{3+}$ as a stoichiometric oxidant with catalyst in buffer, the reaction occurs so quickly that a fast and through mixing is crucial for obtaining meaningful kinetic data. Furthermore, some WOCs have unique early time kinetics which can be obscured by slow mixing, or missed entirely. To this end we developed a system which meets these requirements to facilitate accurate O_2 measurements that reflect the performance of the catalyst and the not speed of mixing.

Although this does not produce kinetics data, the accurate final O_2 yield is still of great use. We have previously been limited by the long instrumental delay required for O_2 quantification in attempts to collect O_2 production kinetics. Thus a second system – dubbed continuous flow – was constructed that by-passes the delay and allows for full kinetic measurement of O_2 production. It also allows for the monitoring of the consumption of $[Ru(bpy)_3]^{3+}$ by UV-vis for same reaction at the same time. This has not been previously reported and nullifies concerns about uniform experimental design when the reactions are separated. Applying data collected from these techniques to a kinetic model which reflects several known side reactions has provided insight to not only the speed of the catalyst, but also the ratio of water oxidation to non-oxygen-producing side reactions. This metric is referred to herein as "selectivity". The kinetic model has also produced good agreement with experiment in terms of kinetic profiles and O_2 yields (compare 0.52 and 0.48 respectively for **Co₄POM**). Knowledge about selectivity is absolutely crucial when considering a WOC for incorporation into a device where lifetime of the system is more important than simply the stability of the catalyst. Work is currently underway to further test the limits of the continuous flow system and adapt it for light-driven reactions.

Acknowledgements

Notes and references

[a] Department of Chemistry, Emory University, 1515 Dickey Drive, Atlanta, GA 30322.

[b] SpectrEcology, Jasper, GA, 30143, United States.

* Corresponding authors: chill@emory.edu and iguelet@emory.edu

† Deriving eq 14 we assumed that $[Ru^{2+}] \approx [Ru^{3+}]_o - [Ru^{3+}]$. The yield, Y, of $[Ru^{2+}]$ per $[Ru^{3+}]_o$ in equation 3 in the absence of catalyst is about 95%. Therefore, it would be reasonably to assume that $[Ru^{2+}] \approx [Ru^{3+}]_o - Y [Ru^{3+}]$. In this case the modified eq 15 predicts that O_2 yield per $[Ru^{3+}]_o$ reaches 95% at high catalyst concentrations.

†† Estimated from the final absorbance of $[Ru^{3+}]$ due to decomposition in the absence of the catalyst as in equation 2.

1. N. D. McDaniel, F. J. Coughlin, L. L. Tinker and S. Bernhard, *J. Am. Chem. Soc.*, 2008, **130**, 210-217.

2. J. T. Muckerman, D. E. Polyansky, T. Wada, K. Tanaka and E. Fujita, *Inorg. Chem.*, 2008, **47**, 1787-1802.

3. J. F. Hull, D. Balcells, J. D. Blakemore, C. D. Incarvito, O. Eisenstein, G. W. Brudvig and R. H. Crabtree, *J. Am. Chem. Soc.*, 2009, **131**, 8730-8731.

4. S. Masaoka and K. Sakai, *Chem. Lett.*, 2009, **38**, 182-183.

5. J. L. Fillol, Z. Codolà, I. Garcia-Bosch, L. Gómez, J. J. Pla and M. Costas, *Nature Chem.*, 2011, **3**, 807-813.

6. S. Roeser, P. Fàrrs, F. Bozoglian, M. Martínez-Belmonte, J. Benet-Buchholz and A. Llobet, *ChemSusChem*, 2011, **4**, 197-207.

7. J. An, L. Duana and L. Sun, *Faraday Discuss.*, 2012, **155**, 267-275.

8. N. Kaveevivitchai, R. Zong, H.-W. Tseng, R. Chitta and R. P. Thummel, *Inorg. Chem.*, 2012, **51**, 2930-2939.

9. M. Murakami, D. Hong, T. Suenobu, S. Yamaguchi, T. Ogura and S. Fukuzumi, *J. Am. Chem. Soc.*, 2011, **133**, 11605-11613.

10. J. J. Stracke and R. G. Finke, *ACS Catal.*, 2014, **4**, 79-89.

11. Y. V. Geletii, B. Botar, P. Kögerler, D. A. Hillesheim, D. G. Musaev and C. L. Hill, *Angew. Chem. Int. Ed.*, 2008, **47**, 3896-3899.

12. S. Goberna-Ferrón, L. Vigara, J. Soriano-López and J. R. Galán-Mascarós, *Inorg. Chem.*, 2012, **51**, 11707-11715.

13. Q. Yin, J. M. Tan, C. Besson, Y. V. Geletii, D. G. Musaev, A. E. Kuznetsov, Z. Luo, K. I. Hardcastle and C. L. Hill, *Science*, 2010, **328**, 342-345.

14. A. Sartorel, M. Carraro, G. Scorrano, R. D. Zorzi, S. Geremia, N. D. McDaniel, S. Bernhard and M. Bonchio, *J. Am. Chem. Soc.*, 2008, **130**, 5006-5007.

15. S. Hoops, S. Sahle, R. Gauges, C. Lee, J. Pahle, N. Simus, M. Singhal, L. Xu, P. Mendes and U. Kummer, *Bioinformatics*, 2006, **22**, 3067-3074.

16. T. Zidki, L. Zhang, V. Shafirovich and S. V. Lymar, *J. Am. Chem. Soc.*, 2012, **134**, 14275-14278.

17. G. Zhu, E. N. Glass, C. Zhao, H. Lv, J. W. Vickers, Y. V. Geletii, D. G. Musaev, J. Song and C. L. Hill, *Dalton Trans.*, 2012, **41**, 13043-13049.

18. M. R. Shahriari, Q. Zhous, J. G.H. Sigel and G. Stokess, Las Vegas, NV, October 1988.

19. W. Wang, C. E. Reimers, M. R. Shahriari and M. J. Morris, *Sea Technology*, March 1999, **40**, 69-74.

20. S. Alla, R. Solanki, Y. D. Mattley, H. Dabhi and M. R. Shahriari, San Jose, CA., February 20, 2009.

21. H. Huang, D. Y. C. Leung and D. Ye, *J. Mater. Chem.*, 2011, **21**, 9647-9652.

22. J. M. Sumliner, J. W. Vickers, H. Lv, Y. V. Geletii and C. L. Hill, in *Molecular Water Oxidation Catalysts: A Key Topic for New Sustainable Energy Conversion Schemes*, ed. A. Llobet, John Wiley & Sons, Ltd., 2014 in press, vol. First Edition, ch. 11, pp. 211-231.

23. A. R. Parent, R. H. Crabtree and G. W. Brudvig, *Chem. Soc. Rev.*, 2013, **42**, 2247-2252.

24. P. K. Ghosh, B. S. Brunschwig, M. Chou, C. Creutz and N. Sutin, *J. Am. Chem. Soc.*, 1984, **106**, 4772-4783.

25. Y. V. Geletii, C. Besson, Y. Hou, Q. Yin, D. G. Musaev, D. Quinonero, R. Cao, K. I. Hardcastle, A. Proust, P. Kögerler and C. L. Hill, *J. Am. Chem. Soc.*, 2009, **131**, 17360-17370.

26. J. Vickers, H. Lv, P. F. Zhuk, Y. V. Geletii and C. L. Hill, *MRS Proceedings*, 2012, **1387**, mrsf11-1387-e1302-1301.

27. J. W. Vickers, H. Lv, J. M. Sumliner, G. Zhu, Z. Luo, D. G. Musaev, Y. V. Geletii and C. L. Hill, *J. Am. Chem. Soc.*, 2013, **135**, 14110-14118.

28. D. R. Anton and R. H. Crabtree, *Organometallics*, 1983, **2**, 855-859.

29. G. M. Whitesides, M. Hackett, R. L. Brainard, J.-P. P. M. Lavalleye, A. F. Sowinski, A. N. Izumi, S. S. Moore, D. W. Brown and E. M. Staudt, *Organometallics*, 1985, **4**, 1819-1830.

30. J. A. Widegren and R. G. Finke, *J. Mol. Catal. A: Chem.*, 2003, **198**, 317-341.

31. J. J. Stracke and R. G. Finke, *ACS Catal.*, 2013, **3**, 1209-1219.

32. J. J. Stracke and R. G. Finke, *J. Am. Chem. Soc.*, 2011, **133**, 14872-14875.

33. A. Juris, V. Balzani, F. Barigelletti, S. Campagna, P. Belser and A. V. Zelewsky, *Coord. Chem. Rev.*, 1988, **84**, 85-277.

34. M. Hara, C. C. Waraksa, J. T. Lean, B. A. Lewis and T. E. Mallouk, *J. Phys. Chem. A*, 2000, **104**, 5275-5280.

35. H. Lv, J. A. Rudd, P. F. Zhuk, J. Y. Lee, E. C. Constable, C. E. Housecroft, C. L. Hill, D. G. Musaev and Y. V. Geletii, *RSC Adv.*, 2013, **3**, 20647-20654.

36. F. Evangelisti, P.-E. Car, O. Blacque and G. R. Patzke, *Catal. Sci. Technol.*, 2013, **3**, 3117-3129.

Table of Contents graphic

A continuous flow reactor for simultaneous measurement of critical early-time concentrations of dioxygen and oxidant in catalytic water oxidation reactions